

Almost perfect blazing by photonic crystal rod gratings

Evgeny Popov, Bozhan Bozhkov, and Michel Nevrière

A periodic array of dielectric rods or holes, known as two-dimensional photonic crystal, is shown to have blazing properties similar to those of classical diffraction gratings. Several different optogeometric configurations are shown numerically to exhibit an almost perfect blazing in the -1 st reflected order with a plateaulike spectral dependence in nonpolarized light. © 2001 Optical Society of America

OCIS codes: 050.7950, 050.1970, 050.2770, 060.4230.

1. Introduction

Since the pioneering work of Yablonovitch,¹ the so-called photonic crystals have been the subject of extensive interest,²⁻⁶ most of it theoretical, at least in the visible region. Only most recently has technological development allowed the production of two-dimensional (2-D) or three-dimensional periodic structures with a characteristic period shorter than the wavelength of visible light.^{7,8}

Most of the attention to photonic crystal diffraction is directed toward structures with subwavelength periods. If d is the period and λ is the wavelength, the Fraunhofer grating equation implies that, when $\lambda/d > 2$, the zeroth order is the only one to be diffracted whatever the incidence. Larger-period structures can diffract light into nonspecular orders, thus complicating the simplified picture of forbidden and allowed bandgaps. The simpler case of specular-only diffraction is common to solid-state physics, where the extensive theoretical investigation of photonic crystals began. However, in optics, nonspecular diffraction has proved for a long time to be quite interesting and useful. Only a few recent studies have dealt with nonspecular diffraction by 2-D photonic crystals,⁹ and the nonzero-order diffraction is not considered in these studies from the point of view of its most important property of diffracting polychromatic light in different directions.

In this paper we propose a numerical study of non-specular light diffraction by a 2-D periodic array of dielectric rods with circular (or rectangular) cross sections. It is shown that within the wavelength band forbidden for transmission, such systems can have almost 100% diffraction efficiency over the entire bandgap in both TE and TM polarization. This perfect blazing can be quite useful for demultiplexing light in optical communication networks by using nonpolarized light transmission. Note that a blazed grating is a grating that concentrates a high amount of energy into a given diffracted order. Thus its absolute efficiency, i.e., the ratio between the diffracted energy in that order and the incident energy, approaches 100%.

A plateaulike almost perfect blazing is known to exist for multilayer diffraction gratings, but only for single polarization, whereas the other polarization efficiency is low and varies rapidly with wavelength.¹⁰⁻¹²

2. System Geometry and Forbidden Band in Transmission

The diffraction system consists of a periodically arranged array of rods (or holes) in a homogeneous material. We consider in-plane diffraction with the plane of incidence and diffraction perpendicular to the rod direction (Fig. 1). The outermost system interfaces are planes that can have different possible directions, i.e., crystal cuts. For example, a system with boundaries parallel to the x axis with a period $d = 1 \mu\text{m}$ can diffract only two diffracted orders for a wavelength λ larger than $2 \mu\text{m}$, namely, the specular order in reflection and the specular transmitted order, whatever the angle of incidence may be. It is well known that in specific conditions such a system can have a forbidden zone in transmission, reflecting back the entire incident light within a given wavelength band. This happens when no system mode is

E. Popov (e.popov@fresnel.fr) and M. Nevrière are with the Laboratoire d'Optique Electromagnétique, Unité de Recherche Associée au Centre National de la Recherche Scientifique 843, Faculté des Sciences et Techniques de St. Jérôme, 13397 Marseille Cedex 20, France. B. Bozhkov is with the Institute of Solid State Physics, 72 Tzarigradsko Chausee Boulevard, 1784 Sofia, Bulgaria.

Received 27 June 2000; revised manuscript received 6 November 2000.

0003-6935/01/152417-06\$15.00/0

© 2001 Optical Society of America

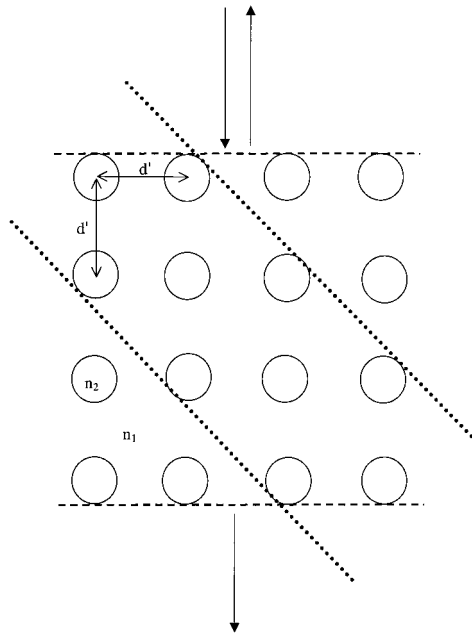


Fig. 1. Schematic representation of the cross section of a periodic system of circular rods: dashed, dotted lines, two different slice cuts; n_1 , n_2 , refractive indices of the bulk material and the rods, respectively.

allowed to propagate without attenuation over a single period of the system in the direction of propagation. Mathematically, such a property can be expressed in terms of the eigenvalues of the transmission matrix of the system, as briefly explained in this section (see the Appendix for more precise proof). Let $F(x,y)$ be the electromagnetic field at point (x,y) inside the system. If we want the system to transmit a portion of the incident light, it is necessary that some phase factor γ (equal to the Bloch vector times the period) with a zero imaginary part exists to link the field at the plane, $y = y_0$ and $y = y_0 + d_y$. Here d_y is the vertical dimension of the single cell of the system:

$$F(x, y_0 + d_y) = \exp(i\gamma) F(x, y_0). \quad (1)$$

On the other hand, the field values at plane $y = y_0$ and $y = y_0 + d_y$ are linked by the transmission matrix, Eq. (A3); thus $\exp(i\gamma)$ equals the eigenvalues of this transmission matrix. When no real γ exists, the system consisting of a sufficient number of identical layers does not transmit light. Spectral (or angular) regions without transmission are called forbidden bands or bandgaps in analogy with solid-state physics. The result is that the bandgaps in transmission will exist in the spectral regions where $\min|\text{Im}(\gamma)| \neq 0$, where $\text{Im}(\gamma)$ denotes the imaginary part of γ .

A typical example of such a gap is shown in Fig. 2. We consider a classical case, as discussed in Ref. 13, of a square array of cylindrical dielectric rods with optical index $n_2 = 2.9833$ ($n_2^2 = 8.9$) hanging in the air ($n_1 = 1$). The vertical period d_y is equal to the horizontal one, equal to $d' = 1 \mu\text{m}$. The crystal is

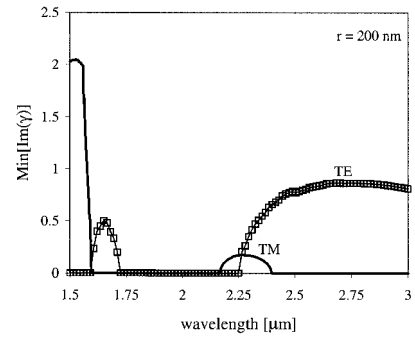


Fig. 2. Spectral dependence of the imaginary part of the eigenvalue of the transmission matrix that has a minimum imaginary part modulus. The slice is cut along the dashed lines in Fig. 1. Solid curve, TM polarization; squares, TE polarization. The band gaps for which $\min|\text{Im}(\gamma)| \neq 0$ are well presented. The system parameters are $d' = 1 \mu\text{m}$, $n_1 = 1$, $n_2 = 2.9833$, $r = 200 \text{ nm}$, incidence normal to the dashed lines in Fig. 1.

cut along the dashed lines in Fig. 1. At normal incidence and rod radii $r = 200 \text{ nm}$, the TE (the electric-field vector parallel to the rods) and TM gaps partially overlap in the wavelength range between 2.25 and 2.32 μm . Calculations for radii r from 50 to 500 nm have shown that greater overlaps occur for $r = 150$ and 350 nm, which is why we shall analyze these two cases in more detail. However, let us first discuss the possible nonspecular diffraction, which does not exist for wavelengths longer than 1 μm and crystal cut along the dashed lines in Fig. 1. Aiming the appearance of diffraction orders rather than the zeroth transmitted and reflected orders, we can choose a crystal cut at 45°, as shown by the dotted lines in Fig. 1, preserving the incident direction. The resulting geometry turned at 45° is presented in Fig. 3. A greater number of degrees of freedom are allowed compared with Fig. 1 by allowing the vertical period to differ from the horizontal period; the radius, the optical index, and the positions of the centers of the rods in the middle layer could also vary. However, in the following we preserve the initial geometry, i.e., $h = d$, $c = h_1 = d/2$.

As the horizontal period is now longer ($d = 1.414 \mu\text{m}$) and the angle of incidence is 45°, another (-1st) diffraction order can propagate in the superstrate and in the substrate for wavelengths shorter than 2.414 μm . Additional orders will appear at shorter wavelengths, but here we are interested in -1st order only. Owing to the different crystal cut, the position of the forbidden gaps is slightly changed. (The results are not shown here.) Their position for two different radii, $r = 350$ and 150 nm, are shown in Fig. 4 for TE and TM polarization. The total reflected light (in the 0th and -1st reflected orders) is drawn as a function of wavelength λ in Fig. 5 where $r = 350 \text{ nm}$ and $M = 10$. (M is the number of vertical periods that form the system; i.e., totally $2M + 1$ layers of rods are involved for the system presented in Fig. 3.) As observed, within the gap, almost (99.9%) of the incident light is reflected in the super-

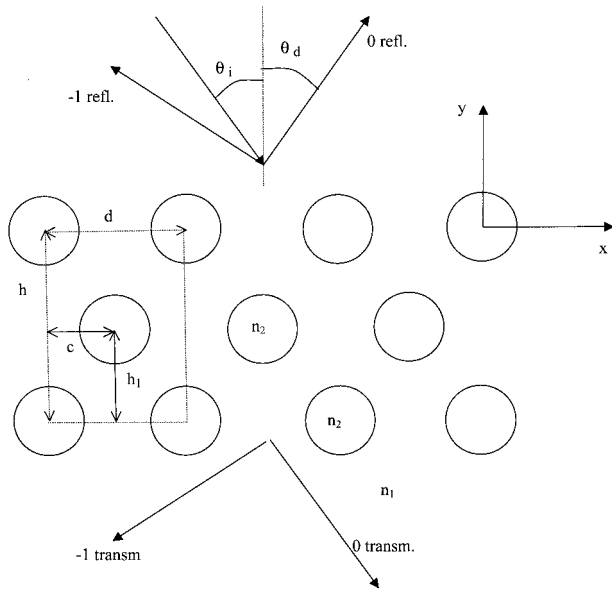


Fig. 3. Schematic representation of a photonic crystal obtained by a cut, as represented by the dotted lines in Fig. 1 and preserving all parameters. Owing to the change in the cut direction, the incidence is changed to 45° and the period is multiplied by $\sqrt{2}$. This permits propagation of the -1 st reflected and transmitted order.

strate. We made the calculations by using the differential method, applied to photonic crystals,^{14,15} which was recently ameliorated to improve the convergence for the TM case.¹⁶ This theory allows one to find the diffracted field as well as the $T^{(1)}$ matrix

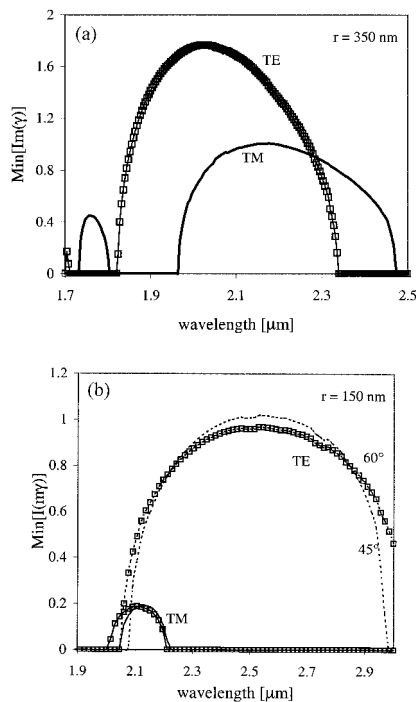


Fig. 4. Forbidden bands for the system in Fig. 3 with $d = h = 1.414 \mu\text{m}$, $c = h_1 = d/2$, $n_1 = 1$, $n_2 = 2.9833$. The polarization is indicated: (a) $r = 350 \text{ nm}$, incidence 45° ; (b) $r = 150 \text{ nm}$; bare lines, 45° incidence; squares, 60° incidence.

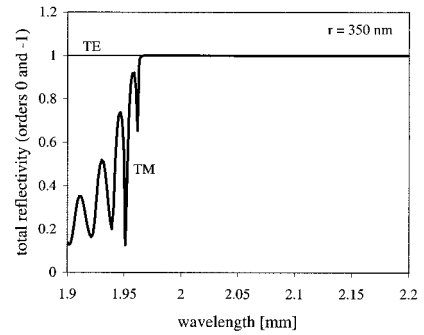


Fig. 5. Total reflected energy (zero and minus first diffracted order) as a function of the wavelength for the system with parameters in Fig. 4(a) and 21 cylinder rows ($M = 10$).

described in the Appendix for any range of optogeometric parameters. When $T^{(1)}$ is known, its eigenvalues can be found by use of standard numerical methods. Note that in our research we fix wavelength λ and the incident angle (i.e., α_0) and search for the vertical component of the wave vector, whereas in solid-state physics the entire wave vector is usually fixed and the frequency is searched.

The gap boundaries do not move significantly when the angle of incidence is changed from 45° to 60° , as observed in Fig. 4(b). However, the fact that no light is transmitted does not ensure that it will go into the

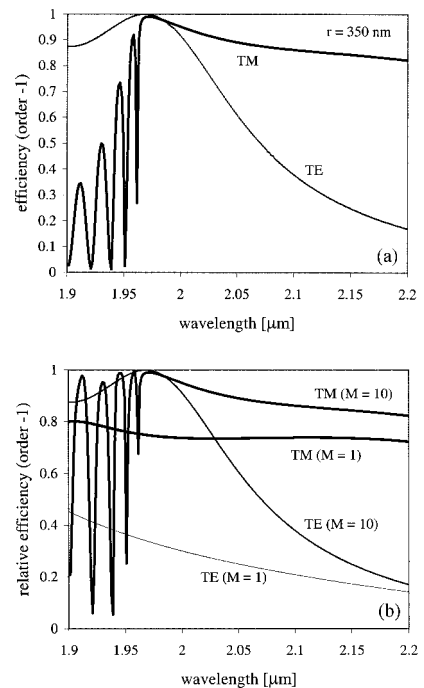


Fig. 6. (a) Spectral dependence of the absolute efficiency in the nonspecular (-1 st) reflected order for the system with parameters in Fig. 4(a) ($r = 350 \text{ nm}$) and 21 rows of rods ($M = 10$). (b) As in (a), but presenting the relative efficiency, defined as the energy diffracted in this order divided by the total reflected energy. The polarization is indicated as well as the number of vertical periods. $M = 1$ corresponds to three layers of rods, whereas $M = 10$ corresponds to 21 layers.

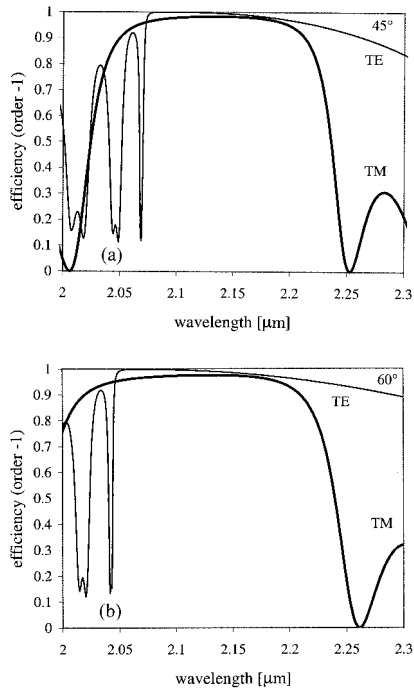


Fig. 7. Spectral dependence of the absolute efficiency in the nonspecular (-1 st) reflected order for the system with parameters in Fig. 4(b) ($r = 150$ nm) and 21 rows of rods ($M = 10$). Angle of incidence: (a) 45° ; (b) 60° .

dispersive -1 st order, since the zeroth reflected order could also carry some energy. Figure 6 shows the spectral dependence of the -1 st-order diffraction efficiency for $r = 350$ nm. Figure 6(a) presents the absolute efficiency for $M = 10$, whereas Fig. 6(b) shows the relative efficiency (energy divided by the total reflected energy) for $M = 10$ and $M = 1$ (only three rows of cylinders). When the TE curves lie entirely inside the gap, the relative and absolute efficiencies for $M = 10$ are equal, which is not the case for $M = 1$ and for TM polarization. The efficiency curves resemble the efficiency curves of a sinusoidal reflecting grating supporting only two diffraction orders. The fact that the spectral behavior of the curves in the gap region is qualitatively the same for $M = 10$ and $M = 1$ (when no vertical periodicity exists) shows that it is determined by the process of

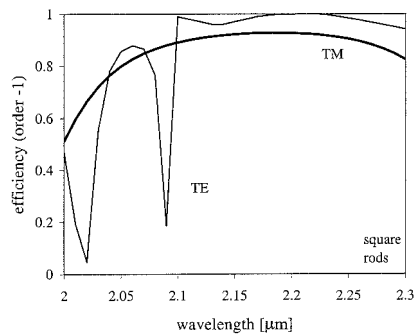


Fig. 8. Same as Fig. 7(a), but with a set of square rods instead of the circular rods. The rods have cross sections of 300×300 nm.

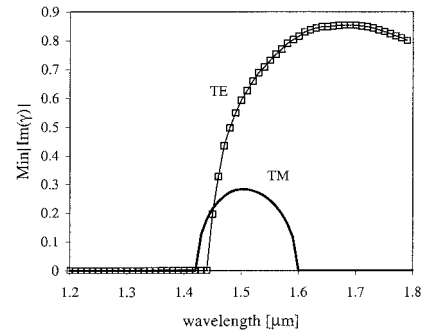


Fig. 9. Forbidden band for the system in Fig. 3 with the following parameters: $d = h = 0.9617$ μm , $c = h_1 = d/2$, $n_1 = 1$, $n_2 = 2.3$, $r = 140$ nm, incidence 45° .

diffraction by a single vertical period plus one additional row (a total of three cylinder rows), whereas the increase of the number of rows leads to a decrease in the transmitted light within the gap. The analogy with a reflection sinusoidal grating¹² is not a mere coincidence, because the grating profile of the cylindrical grating is symmetrical and its filling ratio ($2r/d$) is close to 0.5.

In contrast with the reflection gratings, rod gratings offer a greater number of degrees of freedom. Figure 7 shows the spectral dependence of the absolute diffraction efficiency of the order of -1 when the cylinder radius is reduced to 150 nm. The gap width is slightly reduced (as shown in Fig. 4), but as a reward the diffraction efficiency for both TE and TM polarization forms a plateau 150 nm wide and almost 97% high. The plateau width is larger for 60° inci-

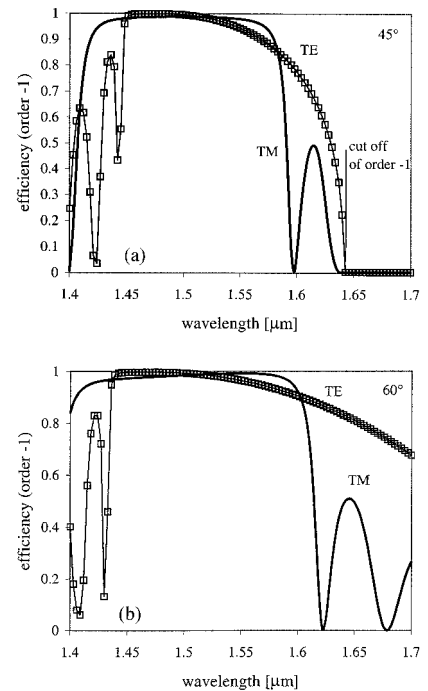


Fig. 10. Spectral dependence of the absolute efficiency in the nonspecular (-1 st) reflected order for the system with parameters in Fig. 9. Angle of incidence: (a) 45° ; (b) 60° .

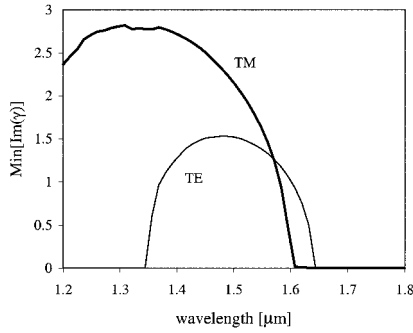


Fig. 11. Forbidden band for a system presented in Fig. 3 with the following parameters: $d = h = 0.38 \mu\text{m}$, $c = h_1 = d/2$, $n_1 = 3.2$, $n_2 = 1$, $r = 80 \text{ nm}$, incidence 60° .

dence [Fig. 7(b)]. Moreover the change in rod geometry does not place undue influence on this blazing property, as shown in Fig. 8 for the same set of rods as in Fig. 3, but with a square cross section with a height and width equal to 300 nm .

This almost perfect blazing in nonpolarized light with a plateaulike spectral dependence can have a great effect on optical communication applications of gratings in demultiplexing. There are two major problems: materials and technology. The next example shows that it is possible to use rods of more conventional optical material (such as lithium niobate) to obtain a blaze window in the desired spectral range of $1.45\text{--}1.6 \mu\text{m}$. To preserve the same number of diffraction orders and angular dispersion, the period in Fig. 3 is reduced to $0.96167 \mu\text{m}$ and the cylinder radii to 140 nm . A mere scanning of the results cannot be applied directly because of dispersion phenomena and new calculations are necessary. The gap and efficiency spectral dependencies are given in Figs. 9 and 10, respectively. As in Fig. 7 the shift from 45° to 60° incidence increases the blaze spectral width and now, in particular, moves the -1st -order cutoff to a longer wavelength.

However, although photonic crystals made of dielectric rods have already been fabricated by diverse technologies, the question of whether it is more desirable to use the inverse configuration remains open. This geometry is characterized by air-filled holes

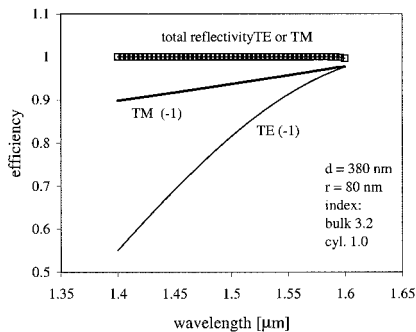


Fig. 12. Diffraction efficiency bare lines, in the reflected -1st order and, squares, the sum of the two reflected orders. The system parameters are as in Fig. 11.

made into a transparent material, usually by use of e-beam lithography.⁹ With the present state of technology the manufactured holes are of finite extent in depth, rarely exceeding $1 \mu\text{m}$, so an analysis needs to take into account the guided-wave phenomena; in our approach we consider a 2-D model with the holes infinitely long in the z direction.

Figure 11 and 12 present the gap region and the efficiency for a 2-D photonic crystal with a bulk index equal to 3.2 , period $d = 380 \text{ nm}$, and the cylindrical holes filled with air. Although the plateaulike blazing region is formed only in TM polarization, the efficiency of TE polarization is relatively high. As for the device studied in Fig. 6, the remaining part of the incident light is reflected into the 0th order, and almost nothing is transmitted inside the gap region.

Appendix A

Let us consider the diffraction system shown in Fig. 1 with outer interfaces parallel to the x axis. If $F(x,y)$ is a solution of Maxwell's equations inside the diffraction system, the pseudo-periodicity of the problem (valid also for inclined incidence) requires that F be quasi-periodic with respect to x :

$$F(x + d, y) = \exp(i\alpha_0 d) F(x, y), \quad (\text{A1})$$

where $\alpha_0 = k \sin \theta_i$, $k = 2\pi n_c / \lambda$ is the modulus of the incident wave vector, n_c is the superstrate optical index, and θ_i is the incidence angle. The direct consequence of Eq. (A1) is that $F(x,y)\exp(-i\alpha_0 x)$ is rigorously periodic with respect to x and thus can be expanded in Fourier series. The expansion for $F(x,y)$ has the form

$$F(x, y) = \exp(i\alpha_0 x) \sum_m F_m(y) \exp(imKx), \quad (\text{A2})$$

where $K = 2\pi/d$ is the grating circular frequency.

The transmission matrix $T^{(1)}$ for one vertical period d_y links the vector \mathbf{F} with components F_m at ordinates y and $y + d_y$:

$$\mathbf{F}(y + d_y) = T^{(1)} \mathbf{F}(y). \quad (\text{A3})$$

The transmission matrix $T^{(1)}$ depends on the basic propagation equation and on the boundary conditions and thus on the polarization. It can be decomposed into three matrices when the eigenvalue technique is used:

$$T^{(1)} = V_T \Phi V_T^{-1}, \quad (\text{A4})$$

where V_T contains the eigenvectors of $T^{(1)}$ and Φ is a diagonal matrix with elements equal to the eigenvalues of $T^{(1)}$. Equation (A3) can be rewritten in another form when Eq. (A4) is used:

$$\tilde{\mathbf{F}}(y + d_y) = \Phi \tilde{\mathbf{F}}(y), \quad (\text{A5})$$

where $\tilde{\mathbf{F}}(y) = V_T^{-1} \mathbf{F}(y)$ is another solution of the Maxwell equations because it is a linear combination of the solutions $\mathbf{F}(y)$. Equation (A5) is similar to Eq. (1). The difference is that in Eq. (A5) Φ is a diagonal

matrix and $\tilde{\mathbf{F}}(\gamma)$ is a vector, whereas F and γ in Eq. (1) are scalars.

The transmission matrix through M vertical periods is simply given by raising the transmission matrix through a single period to the M th power, i.e., by raising the diagonal matrix Φ in Eq. (A5) to power M . The eigenvalues of $T^{(1)}$ can be separated according to the sign of the imaginary part γ'' of γ . The eigenvalues with $\gamma'' > 0$ correspond to field components that propagate and decay exponentially downward; $\gamma'' < 0$ corresponds to solutions that decay exponentially upward. Only solutions with $\gamma'' = 0$ can propagate without decay of their amplitudes.

If no eigenvalue of $T^{(1)}$ exists for which $\gamma'' = 0$, all field components propagating downward with nonzero amplitude on the upper interface will be zero at the lower interface, provided the system contains a sufficient number of layers M so that $\exp(i\gamma M) \approx 0$. The same conclusion is valid for the components propagating upward with nonzero amplitudes on the lower interface. Thus transmission through such a system tends toward zero with the increase in the number of layers, whatever may be the number of propagating diffraction orders in the outermost media.

References

1. E. Yablonovitch, "Inhibited spontaneous emission in solid-state physics and electronics," *Phys. Rev. Lett.* **58**, 2059–2062 (1987).
2. S. John, "Strong localization of photons in certain disordered dielectric superlattices," *Phys. Rev. Lett.* **58**, 2486–2489 (1987).
3. K. Ho, C. Chan, and C. Soukoulis, "Existence of a photonic gap in periodic dielectric structures," *Phys. Rev. Lett.* **65**, 3152–3155 (1990).
4. P. Villeneuve, S. Fan, and J. Joannopoulos, "Microcavities in photonic crystals," in *Microcavities and Photonic Bandgaps*, J. Rarity and C. Weisbuch, eds. (Kluwer Academic, The Netherlands, 1996), pp. 133–151.
5. Z. Zhang and S. Satpathy, "Electromagnetic wave propagation in periodic structures: Bloch wave solution of Maxwell's equations," *Phys. Rev. Lett.* **65**, 2650–2653 (1990).
6. R. Meade, K. Brommer, A. Rappe, and J. Joannopoulos, "Electromagnetic Bloch waves at the surface of a photonic crystal," *Phys. Rev. B* **44**, 10,961–10,964 (1991).
7. T. Krauss, R. De La Rue, and S. Brand, "Two-dimensional photonic-bandgap structures operating at near-infrared wavelengths," *Nature (London)* **383**, 699–702 (1996).
8. D. Labilloy, H. Benisty, C. Weisbuch, T. Krauss, R. Houdré, and U. Oesterle, "Use of guided spontaneous emission of a semiconductor to probe the optical properties of two-dimensional photonic crystals," *Appl. Phys. Lett.* **71**, 738–740 (1997).
9. See, for example, D. Labilloy, H. Benisty, C. Weisbuch, T. Krauss, D. Cassagne, C. Jouanin, R. Houdré, U. Oesterle, and V. Bardinal, "Diffraction efficiency and guided light control by two-dimensional photonic-bandgap lattices," *IEEE J. Quantum Electron.* **35**, 1045–1052 (1999).
10. L. Mashev and E. Popov, "Diffraction efficiency anomalies of multicoated dielectric gratings," *Opt. Commun.* **51**, 131–136 (1984).
11. M. Perry, D. Boyd, J. Britten, B. Shore, C. Shannon, and E. Shults, "High-efficiency multilayer dielectric diffraction gratings," *Opt. Lett.* **20**, 940–942 (1995).
12. E. Loewen and E. Popov, *Diffraction Gratings and Applications* (Marcel Dekker, New York, 1997), Chap. 8.
13. J. Joannopoulos, R. Meade, and J. Winn, *Photonic Crystals* (Princeton University, Princeton, N.J., 1995).
14. P. Vincent, "Differential methods," in *Electromagnetic Theory of Gratings*, R. Petit, ed. (Springer-Verlag, Berlin, 1980), pp. 101–121.
15. E. Popov and B. Bozhkov, "Differential method applied for photonic crystals," *Appl. Opt.* **39**, 4926–4932 (2000).
16. E. Popov and M. Nevière, "Differential theory for diffraction gratings: a new formulation for TM polarization with rapid convergence," *Opt. Lett.* **25**, 598–600 (2000).